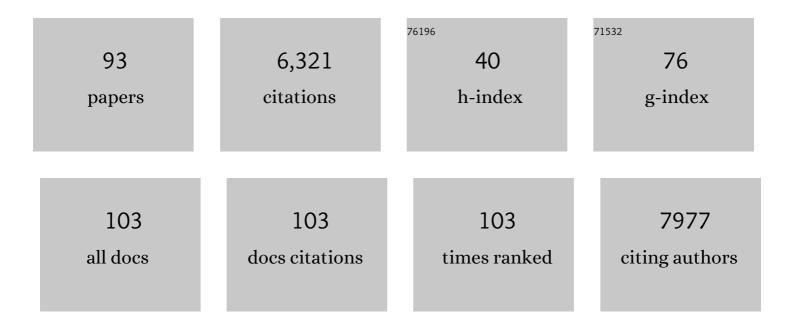
## Kunio Hirata

List of Publications by Year in descending order

Source: https://exaly.com/author-pdf/3109593/publications.pdf Version: 2024-02-01



#	Article	IF	CITATIONS
1	The structure of NLRP9 reveals a unique Câ€ŧerminal region with putative regulatory function. FEBS Letters, 2022, 596, 876-885.	1.3	4
2	Molecular mechanism of agonism and inverse agonism in ghrelin receptor. Nature Communications, 2022, 13, 300.	5.8	18
3	Macromolecular Crystallography at SPring-8. Nihon Kessho Gakkaishi, 2022, 64, 2-9.	0.0	0
4	Crystal structure of Tam41 cytidine diphosphate diacylglycerol synthase from a Firmicutes bacterium. Journal of Biochemistry, 2022, 171, 429-441.	0.9	1
5	Binding pathway determines norepinephrine selectivity for the human β1AR over β2AR. Cell Research, 2021, 31, 569-579.	5.7	65
6	An unprecedented insight into the catalytic mechanism of copper nitrite reductase from atomic-resolution and damage-free structures. Science Advances, 2021, 7, .	4.7	25
7	<i>In-Cell</i> Engineering of Protein Crystals with Nanoporous Structures for Promoting Cascade Reactions. ACS Applied Nano Materials, 2021, 4, 1672-1681.	2.4	21
8	Design of an Inâ€Cell Protein Crystal for the Environmentally Responsive Construction of a Supramolecular Filament. Angewandte Chemie - International Edition, 2021, 60, 12341-12345.	7.2	13
9	Design of an Inâ€Cell Protein Crystal for the Environmentally Responsive Construction of a Supramolecular Filament. Angewandte Chemie, 2021, 133, 12449-12453.	1.6	0
10	XFEL Crystal Structures of Peroxidase Compound II. Angewandte Chemie - International Edition, 2021, 60, 14578-14585.	7.2	18
11	XFEL Crystal Structures of Peroxidase Compound II. Angewandte Chemie, 2021, 133, 14699-14706.	1.6	0
12	Short-lived intermediate in N <sub>2</sub> O generation by P450 NO reductase captured by time-resolved IR spectroscopy and XFEL crystallography. Proceedings of the National Academy of Sciences of the United States of America, 2021, 118, .	3.3	21
13	Endogenous agonist–bound S1PR3 structure reveals determinants of G protein–subtype bias. Science Advances, 2021, 7, .	4.7	31
14	Guidelines for <i>de novo</i> phasing using multiple small-wedge data collection. Journal of Synchrotron Radiation, 2021, 28, 1284-1295.	1.0	7
15	The structure of an archaeal oligosaccharyltransferase provides insight into the strict exclusion of proline from the N-glycosylation sequon. Communications Biology, 2021, 4, 941.	2.0	4
16	The Crystal Structure of Angiotensin II Type 2 Receptor with Endogenous Peptide Hormone. Structure, 2020, 28, 418-425.e4.	1.6	40
17	Structural Basis for Blocking Sugar Uptake into the Malaria Parasite Plasmodium falciparum. Cell, 2020, 183, 258-268.e12.	13.5	42
18	Ribosomal synthesis and de novo discovery of bioactive foldamer peptides containing cyclic β-amino acids. Nature Chemistry, 2020, 12, 1081-1088.	6.6	86

Kunio Hirata

#	Article	IF	CITATIONS
19	Structure of an antagonist-bound ghrelin receptor reveals possible ghrelin recognition mode. Nature Communications, 2020, 11, 4160.	5.8	55
20	lsoprenoid-chained lipid EROCOC17+4: a new matrix for membrane protein crystallization and a crystal delivery medium in serial femtosecond crystallography. Scientific Reports, 2020, 10, 19305.	1.6	16
21	An allosteric modulator binds to a conformational hub in the β2 adrenergic receptor. Nature Chemical Biology, 2020, 16, 749-755.	3.9	51
22	Isoform-selective regulation of mammalian cryptochromes. Nature Chemical Biology, 2020, 16, 676-685.	3.9	61
23	Computer-controlled liquid-nitrogen drizzling device for removing frost from cryopreserved crystals. Acta Crystallographica Section F, Structural Biology Communications, 2020, 76, 616-622.	0.4	5
24	Catalytically important damage-free structures of a copper nitrite reductase obtained by femtosecond X-ray laser and room-temperature neutron crystallography. IUCrJ, 2019, 6, 761-772.	1.0	24
25	Mechanism of β <sub>2</sub> AR regulation by an intracellular positive allosteric modulator. Science, 2019, 364, 1283-1287.	6.0	82
26	An oxyl/oxo mechanism for oxygen-oxygen coupling in PSII revealed by an x-ray free-electron laser. Science, 2019, 366, 334-338.	6.0	248
27	Structures of the 5-HT2A receptor in complex with the antipsychotics risperidone and zotepine. Nature Structural and Molecular Biology, 2019, 26, 121-128.	3.6	133
28	Crystal structure of the M <sub>5</sub> muscarinic acetylcholine receptor. Proceedings of the National Academy of Sciences of the United States of America, 2019, 116, 26001-26007.	3.3	48
29	Ligand binding to human prostaglandin E receptor EP4 at the lipid-bilayer interface. Nature Chemical Biology, 2019, 15, 18-26.	3.9	85
30	Crystal structure of the endogenous agonist-bound prostanoid receptor EP3. Nature Chemical Biology, 2019, 15, 8-10.	3.9	49
31	<i>ZOO</i> : an automatic data-collection system for high-throughput structure analysis in protein microcrystallography. Acta Crystallographica Section D: Structural Biology, 2019, 75, 138-150.	1.1	156
32	Data Collection Strategy in Protein Micro-crystallography at Synchrotron Facility. Seibutsu Butsuri, 2019, 59, 215-218.	0.0	0
33	Remodeling of the optics for a micro-focusing protein crystallography beamline at SPring-8. , 2019, , .		0
34	Supramolecular protein cages constructed from a crystalline protein matrix. Chemical Communications, 2018, 54, 1988-1991.	2.2	10
35	Na+-mimicking ligands stabilize the inactive state of leukotriene B4 receptor BLT1. Nature Chemical Biology, 2018, 14, 262-269.	3.9	80
36	Structure of in cell protein crystals containing organometallic complexes. Physical Chemistry Chemical Physics, 2018, 20, 2986-2989.	1.3	5

KUNIO HIRATA

#	Article	IF	CITATIONS
37	Crystal structures of human ETB receptor provide mechanistic insight into receptor activation and partial activation. Nature Communications, 2018, 9, 4711.	5.8	60
38	Structural insights into the subtype-selective antagonist binding to the M2 muscarinic receptor. Nature Chemical Biology, 2018, 14, 1150-1158.	3.9	59
39	Structure-guided development of selective M3 muscarinic acetylcholine receptor antagonists. Proceedings of the National Academy of Sciences of the United States of America, 2018, 115, 12046-12050.	3.3	64
40	Crystal structure of the human angiotensin II type 2 receptor bound to an angiotensin II analog. Nature Structural and Molecular Biology, 2018, 25, 570-576.	3.6	58
41	Structural basis for promotion of duodenal iron absorption by enteric ferric reductase with ascorbate. Communications Biology, 2018, 1, 120.	2.0	30
42	An unprecedented dioxygen species revealed by serial femtosecond rotation crystallography in copper nitrite reductase. IUCrJ, 2018, 5, 22-31.	1.0	27
43	<i>KAMO</i> : towards automated data processing for microcrystals. Acta Crystallographica Section D: Structural Biology, 2018, 74, 441-449.	1.1	198
44	Crystal Engineering of Self-Assembled Porous Protein Materials in Living Cells. ACS Nano, 2017, 11, 2410-2419.	7.3	53
45	Development of a dose-limiting data collection strategy for serial synchrotron rotation crystallography. Journal of Synchrotron Radiation, 2017, 24, 29-41.	1.0	39
46	A nanosecond time-resolved XFEL analysis of structural changes associated with CO release from cytochrome c oxidase. Science Advances, 2017, 3, e1603042.	4.7	68
47	Structural insights into ligand recognition by the lysophosphatidic acid receptor LPA6. Nature, 2017, 548, 356-360.	13.7	101
48	X-ray structures of endothelin ETB receptor bound to clinical antagonist bosentan and its analog. Nature Structural and Molecular Biology, 2017, 24, 758-764.	3.6	79
49	Structural basis for xenobiotic extrusion by eukaryotic MATE transporter. Nature Communications, 2017, 8, 1633.	5.8	69
50	Capturing an initial intermediate during the P450nor enzymatic reaction using time-resolved XFEL crystallography and caged-substrate. Nature Communications, 2017, 8, 1585.	5.8	74
51	Protein microcrystallography using synchrotron radiation. IUCrJ, 2017, 4, 529-539.	1.0	56
52	Remote access and automation of SPring-8 MX beamlines. AIP Conference Proceedings, 2016, , .	0.3	23
53	Structural Biology with Microfocus Beamlines. Springer Protocols, 2016, , 241-273.	0.1	7
54	Cell-free methods to produce structurally intact mammalian membrane proteins. Scientific Reports, 2016, 6, 30442.	1.6	56

Kunio Hirata

#	Article	IF	CITATIONS
55	Structural basis for disruption of claudin assembly in tight junctions by an enterotoxin. Scientific Reports, 2016, 6, 33632.	1.6	85
56	Redox-coupled structural changes in nitrite reductase revealed by serial femtosecond and microfocus crystallography. Journal of Biochemistry, 2016, 159, 527-538.	0.9	26
57	Automated system for data collection and data processing using microcrystals. Acta Crystallographica Section A: Foundations and Advances, 2015, 71, s187-s187.	0.0	0
58	High-resolution native structure analyses of supramacromolecular complexes susceptible to radiation damage. Acta Crystallographica Section A: Foundations and Advances, 2015, 71, s15-s15.	0.0	0
59	Determination of Radiation Damage-free Crystal Structure of Cytochrome <i>c</i> Oxidase Using XFEL. Seibutsu Butsuri, 2015, 55, 084-086.	0.0	1
60	Determination of Damage-free Crystal Structure of an X-ray Sensitive Protein Using XFEL. Nihon Kessho Gakkaishi, 2015, 57, 122-128.	0.0	158
61	Design of Enzymeâ€Encapsulated Protein Containers by In Vivo Crystal Engineering. Advanced Materials, 2015, 27, 7951-7956.	11.1	32
62	Atomistic design of microbial opsin-based blue-shifted optogenetics tools. Nature Communications, 2015, 6, 7177.	5.8	78
63	Expression, purification, crystallization, and preliminary X-ray crystallographic studies of the human adiponectin receptors, AdipoR1 and AdipoR2. Journal of Structural and Functional Genomics, 2015, 16, 11-23.	1.2	14
64	Molecular basis of ligand recognition and transport by glucose transporters. Nature, 2015, 526, 391-396.	13.7	305
65	A magnetic anti-cancer compound for magnet-guided delivery and magnetic resonance imaging. Scientific Reports, 2015, 5, 9194.	1.6	40
66	Crystal structures of the human adiponectin receptors. Nature, 2015, 520, 312-316.	13.7	176
67	Native structure of photosystem II at 1.95ÂÃ resolution viewed by femtosecond X-ray pulses. Nature, 2015, 517, 99-103.	13.7	1,050
68	Crystal structure of a bacterial homologue of SWEET transporters. Cell Research, 2014, 24, 1486-1489.	5.7	71
69	Crystallization and preliminary X-ray diffraction analysis of YidC, a membrane-protein chaperone and insertase from <i>Bacillus halodurans</i> . Acta Crystallographica Section F, Structural Biology Communications, 2014, 70, 1056-1060.	0.4	11
70	Structural basis of Sec-independent membrane protein insertion by YidC. Nature, 2014, 509, 516-520.	13.7	203
71	Determination of damage-free crystal structure of an X-ray–sensitive protein using an XFEL. Nature Methods, 2014, 11, 734-736.	9.0	237
72	Structural Basis for the Counter-Transport Mechanism of a H <sup>+</sup> /Ca <sup>2+</sup> Exchanger. Science, 2013, 341, 168-172.	6.0	73

IF # ARTICLE CITATIONS Achievement of protein micro-crystallography at SPring-8 beamline BL32XU. Journal of Physics: Conference Series, 2013, 425, 012002 SPring-8 BL41XU, a high-flux macromolecular crystallography beamline. Journal of Synchrotron 74 1.0 25 Radiation, 2013, 20, 910-913. 1P034 Structural Basis for the Counter-Transport Mechanism of a H^+/Ca^<2+> Exchanger(01B.) Tj ETQq1 1 0.784314 rgBT /Overloc Crystal structure of the channelrhodopsin light-gated cation channel. Nature, 2012, 482, 369-374. 76 13.7 503 Fine-needle capillary mounting for protein microcrystals. Journal of Applied Crystallography, 2012, 45, 1.9 785-788. Expression, purification and preliminary X-ray crystallographic analysis of cyanobacterial biliverdin reductase. Acta Crystallographica Section F: Structural Biology Communications, 2011, 67, 313-317. 78 0.7 4 Present status of SPring-8 macromolecular crystallography beamlines. AIP Conference Proceedings, 79 0.3 2010,,. New micro-beam beamline at SPring-8, targeting at protein micro-crystallography. AIP Conference 80 0.3 18 Proceedings, 2010, , . A peroxide bridge between Fe and Cu ions in the O <sub>2</sub> reduction site of fully oxidized cytochrome <i>c</i> oxidase could suppress the proton pump. Proceedings of the National Academy of 3.3 132 Sciences of the United States of America, 2009, 106, 2165-2169. Design optimization of highly accurate elliptical mirrors for hard-x-ray microfocusing probes at 82 14 SPring-8., 2009, , . Crystallization and preliminary X-ray analysis of the stress-response PPM phosphatase RsbX frómBacillus subtilis. Acta Crýstallographica Section F: Structural Biology Communications, 2009, 65, 0.7 1128-1130. Development of a shutterless continuous rotation method using an X-ray CMOS detector for protein 84 1.9 19 crystallography. Journal of Applied Crystallography, 2009, 42, 1165-1175. Process of Accumulation of Metal lons on the Interior Surface of apo-Ferritin: Crystal Structures of a Series of apo-Ferritins Containing Variable Quantities of Pd(II) Ions. Journal of the American Chemical Society, 2009, 131, 5094-5100. 6.6 88 Polymerization of Phenylacetylene by Rhodium Complexes within a Discrete Space of apo-Ferritin. 86 6.6 165 Journal of the American Chemical Society, 2009, 131, 6958-6960. S11.17 A peroxide bridge between the two metals in the dinuclear center of the fully oxidized cytochrome c oxidase. Biochimica Et Biophysica Acta - Bioenergetics, 2008, 1777, S69. Radiation Damage of Protein Crystal in Various X-ray Energies. AIP Conference Proceedings, 2007, , . 88 0.3 1 1P067 The micro-focus beamline to open the new field of protein micro-crystallography(Proteins-functions, methodology, and protein enigineering, Oral) Tj ETQq1 1 0.784314 rgBT / @verlock to Tf 50

**KUNIO HIRATA** 

<sup>90</sup> Dose dependence of radiation damage for protein crystals studied at various X-ray energies. Journal of Synchrotron Radiation, 2007, 14, 4-10.

#	Article	IF	CITATIONS
01	2P026 Current Status of Public Beamlines for Protein Crystallography at SPring-8(29. Protein) Tj ETQq1 1 0.7843		
91	Butsuri, 2006, 46, S302.	0.0	Ο
92	Crystallization and X-ray diffraction analysis of a catalytic domain of hyperthermophilic chitinase fromPyrococcus furiosus. Acta Crystallographica Section F: Structural Biology Communications, 2006, 62, 791-793.	0.7	6
93	Scaling of one-shot oscillation images with a reference data set. Journal of Synchrotron Radiation, 2004, 11, 60-63.	1.0	2